A probable $Na^+(K^+)/H^+$ exchanger on the chloroplast envelope functions in pH homeostasis and chloroplast development in *Arabidopsis thaliana*

Chun-Peng Song*†, Yan Guo*, Quansheng Qiu*, Georgina Lambert*, David W. Galbraith*, André Jagendorf‡, and Jian-Kang Zhu*§¶

*Department of Plant Sciences, University of Arizona, Tucson, AZ 85721; ‡Department of Plant Biology, Cornell University, Ithaca, NY 14853; and §Institute for Integrative Genome Biology and Department of Botany and Plant Sciences, University of California, Riverside, CA 92521

Contributed by André Jagendorf, May 26, 2004

Electroneutral monovalent cation/proton antiport across the chloroplast envelope has been shown previously to have an important regulatory effect on stromal pH and thereby on photosynthetic carbon reduction. Here we report that an *Arabidopsis* nuclear gene, *AtCHX23*, encodes a putative $Na^+(K^+)/H^+$ exchanger and functions in the adjustment of pH in the cytosol and possibly in maintaining a high pH level in the chloroplast stroma. The AtCHX23 protein is localized in the chloroplast envelope. Plastids from *chx23* mutants had straight thylakoids but lacked grana lamellae. *chx23* mutant leaves were pale yellow and had a much reduced chlorophyll content. The chlorophyll content of *chx23* was increased by growing in medium at low (4.0) pH and decreased by growing at high (7.0) pH. The cytosolic pH in the leaves of the mutant was significantly higher than that in the wild type. *chx23* mutants displayed a high sensitivity to NaCl. Together, these data indicate that CHX23 is a probable chloroplast $Na^+(K^+)/H^+$ exchanger important for pH homeostasis and chloroplast development and function.

The chemiosmotic theory of energy transduction across the chloroplast thylakoid membrane postulated that a pH gradient between the stroma and the thylakoid lumen, developed under illumination, drives ATP synthesis (1). Subsequently, Jagendorf and Uribe (2) showed that chloroplast thylakoid vesicles synthesized ATP in the dark when subjected to an abrupt shift of pH. Stromal pH somewhat depends on external pH as well as on proton uptake by thylakoids in the light. The light-induced stromal alkalization is quickly reversed in the dark as protons passively diffuse across the membrane from the thylakoid lumen. The high stromal pH (alkalization) induced by light is a critical regulator of several enzymes of the photosynthetic carbon reduction cycle (3) and facilitates optimal photosynthesis (4).

The stromal pH of illuminated chloroplasts is close to 8.0 (3, 4), whereas cytoplasmic pH is maintained at ≈7.0 (3–5). The question of how the high stromal pH is maintained next to a much lower cytosolic pH has been posed since the 1970s. It was well known that the chloroplast inner envelope is impermeable to protons (4). Electroneutral monovalent cation/proton antiport across the chloroplast envelope was shown to have a strong effect on the chloroplast stroma pH and could thereby either help or inhibit photosynthesis (6, 7). Subsequent work (8, 9) indicated the existence of a complex regulatory system, including a monovalent cation/proton antiporter, monovalent cation channels, and ATPase-dependent H^+ efflux, across the chloroplast envelope. However, none of the hypothesized chloroplast envelope transporters have been identified as yet.

Na^+/H^+ antiporters are ubiquitous membrane proteins that play important roles in signal transduction and in the regulation of ion and pH homeostasis, cell volume, and cell energetics (10). They exist in the plasmalemma and organellar membranes of cells of diverse organisms (11–14), including bacteria, animals, and plants. The *Arabidopsis* Na^+/H^+ antiporter AtNHX1 was identified based on its sequence similarity to the *Saccharomyces cerevisiae* NHX1 (15). Plant NHX1 functions in compartmentalization of Na^+ and also K^+ into vacuoles (16), and in maintaining vacuolar pH homeostasis (12). In the Japanese morning glory (*Ipomoea nil* or *Pharbitis nil*), a shift from reddish-purple buds to blue open flowers correlates with an increase in the vacuolar pH. A mutant purple-flower Japanese morning glory (*I. nil*) carries a recessive mutation in the gene encoding a vacuolar $Na^+(K^+)/H^+$ exchanger; therefore it is unable to increase its vacuolar pH to create the normal bright blue petals (12, 17). The *Arabidopsis SOS1* gene encodes a plasma membrane Na^+/H^+ antiporter (14, 18). SOS1 functions in Na^+ efflux across the plasma membrane, and it controls long-distance Na^+ transport from root to shoot (19).

The *Arabidopsis* genome encodes many putative $Na^+(K^+)/H^+$ antiporters (20). The multiplicity of putative plant $Na^+(K^+)/H^+$ antiporters might reflect various development- and/or stress-specific requirements for Na^+ or K^+ transport. Volume and osmotic regulation in organellar biogenesis and pH homeostasis may be additional functions for the putative Na^+/H^+ antiporters. Here, we report that one of the putative $Na^+(K^+)/H^+$ antiporter genes, *AtCHX23* (20), encodes a plastid envelope protein and functions in the appropriate adjustment of pH in the chloroplast and cytoplasm. The cytosolic pH in the yellow leaves of *chx23* mutant plants was significantly higher than in wild-type leaves. Our results suggest that AtCHX23 controls chloroplast development and plant salt tolerance, perhaps through its role in regulating the homeostasis of cytoplasmic and stromal pH and Na^+ concentration.

Materials and Methods

Strategy for Production of Double-Stranded RNAs (dsRNAs) and Plant Transformation. A gene-specific cDNA fragment of *AtCHX23* was amplified by PCR by using the following primer pairs: forward primer 5′- CGGGATCCATTTAAATGACCCATGTGCACAAATCAG-3′ and reverse primer 5′-GGACTAGTGGCGCGCCCACGTTTCATAATCGCACATG-3′. The forward primer contains *Bam*HI and *Swa*I restriction sites, and the reverse primer contains *Spe*I and *Asc*I restriction sites that are underlined. The resulting PCR product was digested with *Asc*I and *Swa*I and ligated to the *Asc*I and *Swa*I-cleaved vector pFGC1008 (http://www.chromdb.org). The cloned fragment was sequenced to ensure that the correct cDNA was amplified and cloned. This plasmid served as a template to generate a second PCR fragment with which to complete the inverted

Abbreviations: GUS, β-glucuronidase; BCECF-AM, 2′,7′-bis-(2-carboxyethyl)-5-(and-6)-carboxyfluorescein acetoxymethyl ester; RNAi, RNA-mediated interference; MS medium, Murashige and Skoog medium.

†Present address: Department of Biology, Henan University, Kaifeng 475001, China.

¶To whom correspondence should be addressed. E-mail: jian-kang.zhu@ucr.edu.

repeat construct. (The primers for the second PCR step are the same 5′ and 3′ primers originally used to amplify the first PCR fragment.) This time, the PCR fragment was cleaved with *Bam*HI and *Xba*I and inserted into the *Bam*HI-*Xba*I sites of the template plasmid, producing an inverted repeat interrupted by the 335-bp β-glucuronidase (GUS) sequence. The dsRNA construct was introduced into *Agrobacterium tumefaciens* strain GV3101 and transformed into wild-type (Columbia ecotype) plants by floral infiltration.

Histochemical Analysis of GUS Activity. A DNA fragment containing 1.6 kb of the upstream region of the *AtCHX23* was amplified by PCR by using oligonucleotides incorporating *Bam*H1 and *Sal*I sites. The PCR fragments were digested with *Bam*H1 and *Sal*I and then cloned into the *Sal*I-*Bam*H1 site of promoterless GUS expression vector, pCMB1301. The construct, *AtCHX23-GUS*, was transferred from *Escherichia coli* DH5α into *A. tumefaciens* GV3101. *Arabidopsis* was transformed by flower infiltration with *Agrobacterium* that contained *AtCHX23* promoter-*GUS*. Histochemical localization of GUS activities in the transgenic plants was observed by incubating them in 5-bromo-4-chloro-3-indolyl glucuronide (X-gluc) buffer (50 mM sodium phosphate buffer, pH 7.0/10 mM EDTA/0.1% Triton X-100/0.5 mM potassium ferrocyanide/2 mg·ml^{-1} X-gluc) at 37°C for 12 h.

RT-PCR Analysis. Total RNA isolated from 2-week-old seedlings of wild-type and *chx23* (independent transformants #14 and #20) plants was used as template for reverse transcription, by using the SuperScript preamplification system for first-strand cDNA synthesis (GIBCO/BRL) for 50 min at 42°C. After completion of first-strand cDNA synthesis, 1-μl aliquots were taken for PCR detection of transcripts by using the forward primer of *chx23* and reverse primer AATTCCATATTGATGATCCTCTTC for RNA-mediated interference (RNAi) construction. The reverse primer sequence is not present in the gene-specific *AtCHX23* fragment in the RNAi construct, and therefore it amplifies only the respective gene transcript. The reaction mixture (25-μl volume) contained 1 × PCR buffer, 2 mM $MgCl_2$, 0.2 mM dNTPs, 1.2 units of *Taq* polymerase, and 0.2 μM each of above primer pairs. PCR comprised 30 cycles of 94°C for 1 min, 55°C for 1 min, and 72°C for 1 min. Cycling was preceded by an initial denaturation step (94°C for 2 min) and followed by a final extension step (72°C for 10 min). The amplification products were then analyzed by 1% agarose gel electrophoresis.

Subcellular Localization of the AtCHX23-GFP Fusion Protein. The GFP gene was fused in frame to AtCHX23 at its C terminus. The AtCHX23 gene was amplified by using the following primers: GACTCGAGATGTCTTCCGGAGCCCCCCTTAATGTGACA and ACAAGCTTCCTATGAATTCCATATTGATGATCCTCTTC. The PCR fragment was inserted in plasmid pEZTNL, and the resulting construct was introduced into *A. tumefaciens* strain LB4404. *Arabidopsis thaliana* (ecotype Columbia) wild-type plants were transformed. Thirty independent transgenic lines were used for localization of the fusion protein. GFP was visualized by using a Bio-Rad 1024 (Hercules, CA) confocal scanning head attached to a Nikon (Tokyo) Optiphot 2 microscope.

Callus Culture. Wild-type and *chx23 Arabidopsis* calli were induced from hypocotyl explants. After induction, calli were transferred to a multiplication medium composed of Murashige and Skoog medium (MS) basal salts (21), 1 mg/liter 2,4-dichlorophenoxyacetic acid, 10 μg/liter kinetin, 3% sucrose, and 0.8% agar, with or without 100 mM NaCl, and grew in this medium for 24 days at 25°C in the dark. The callus growth was quantified in terms of relative growth rate measured by the $(m_f - m_i)/m_i$ ratio, where m_f was the fresh weight of calli at 24 d culture and m_i, their fresh weight at time of transfer.

Envelope and Thylakoid Purifications. Chloroplasts were isolated from leaves of wild-type and transgenic lines containing pEGAD-CHX23 and purified by Percoll gradients (22). Chloroplasts were hypotonically lysed, and the sample was layered on top of the sucrose layers of 0.45 M and 1 M. Stroma, envelopes, and thylakoids were separated by centrifugation at 90,000 × *g* for 2 h (23).

Loading in Plant Cells with BCECF-AM. The pH-sensitive dye 2′, 7′-bis-(2-carboxyethyl)-5-(and-6)-carboxyfluorescein acetoxymethyl ester (BCECF-AM) (Molecular Probes) was prepared as a 1 mM stock solution in DMSO. Leaves of *Arabidopsis* were submerged in a loading buffer (1 mM KCl/1 mM Mes/0.1 mM $CaCl_2$/0.05% Pluronic F-127) containing 2 μM BCECF-AM and shaken slowly for 15 min in the dark at 25°C.

Ratiometric Measurement of Cytoplasmic pH. The fluorescence images of the pH-sensitive dye BCECF in guard cells were obtained by pseudoratiometric confocal imaging. Dual-excitation confocal ratio measurements used a confocal laser scanning microscope based on a Bio-Rad MRC2400 attached to a Nikon Diaphot inverted microscope with modification of the excitation path to receive coaligned beams at 488 nm (25 mW argon ion) and 442 nm.

Confocal fluorescence optical sections were collected from guard cells and protoplast suspensions by using sequential excitation at 442 and 488 nm and emission at 520 ± 10 nm (power 30%, zoom 4, mild scanning, frame 512 × 512) with pixel spacing of 0.183–0.25 μm. To extract quantitative data, pixel values were averaged over rectangular regions (4 μm^2) manually located on each wavelength image. A single ratio value was calculated from the average 488 intensity, divided by the average 442 intensity for this region, after subtraction of the corresponding image backgrounds.

Calibrations of Ratio Values. *In vitro* calibration was performed by using 10 μM BCECF in a pseudocytoplasm (100 mM KCl/10 mM NaCl/1 mM $MgSO_4$/10 mM Mes/10 mM Hepes, adjusted with Tris base to the desired pH). *In situ* calibration was performed by using 10 μg/ml nigericin and 100 mM KCl (24, 25) to equilibrate the intracellular pH with the controlled extracellular medium.

Electron Microscopy. Scanning electron microscopy observations were made by using a Leica (Wetzlar, Germany) microscope. Two-week-old seedling of wild-type and *chx23* mutant seedlings grown on the surface of MS agar medium were fixed *in situ* on the agar plates by using 2.5% glutaraldehyde in MS solution and postfixed with 1% osmium tetroxide in water. After dehydration and critical point drying, the samples were attached to stubs, coated with gold, and examined by scanning electron microscopy.

Results

AtCHX23 Is a Putative $Na^+(K^+)/H^+$ Antiporter on the Chloroplast Envelope. SOS1 is a transmembrane protein with similarities to plasma membrane Na^+/H^+ antiporters from bacteria and fungi (14). It is involved in Na^+ and K^+ homeostasis of cells and is essential for plant salt tolerance. A BLAST search with SOS1 identified several putative Na^+/H^+ antiporters from the *Arabidopsis* genome database. One of them, classified as AtCHX23 (20), was chosen for functional analysis. The *AtCHX23* gene is located on chromosome I (At1g05580) and encodes a protein of 867-aa residues with a predicted molecular mass of 95.8 kDa. The N-terminal half of AtCHX23 has 12 predicated transmem-

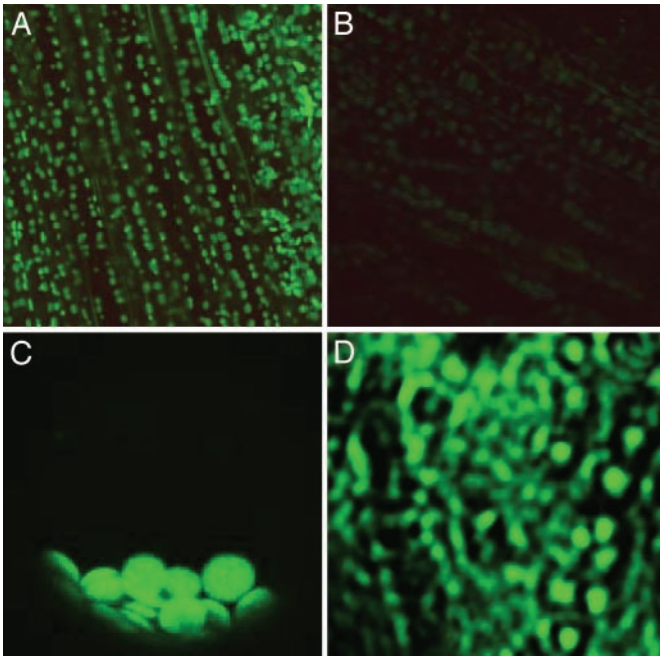

Fig. 1. Subcellular localization of the AtCHX23-GFP fusion protein. (*A*) Chloroplast localization of AtCHX23-GFP in cells from main vein and leaves. (*B*) Autofluorescence of leaf cells under same conditions as in *A*. (*C*) A single protoplast isolated from the transgenic lines with pEZTL-CHX23-GFP. The protoplast had been centrifuged, so the chloroplasts are bunched together at the bottom. (*D*) The chloroplast envelope membrane vesicles purified from AtCHX23-GFP transgenic plants.

brane domains according to PSORT prediction (http://psort.nibb.ac.jp/form.html). Phylogenetic analysis indicates there is a close relationship among AtCHX23, NhaS3, and NhaS4 from the cyanobacterium *Synechocystis* (26) (data not shown). AtCHX23 has 22% identity and 43% similarity with NhaS3 over a stretch of 217 aa (113–440 in AtCHX23). The C-terminal region of AtCHX23 does not show substantial similarity to proteins of known function (data not shown).

To determine the subcellular localization of AtCHX23, a translational fusion of AtCHX23 and the GFP was expressed under the control of the cauliflower mosaic virus 35S promoter in transgenic *Arabidopsis* plants. As shown in Fig. 1*A*, the green fluorescence signal of AtCHX23-GFP was found in chloroplasts. The background green fluorescence from the chloroplasts in untransformed plants was very weak (Fig. 1*B*). In an intact protoplast from AtCHX23-GFP transgenic leaves, green fluorescence was clearly seen in chloroplasts (Fig. 1*C*) but not in any other organelles. We isolated the chloroplast envelope and the thylakoid membranes from protoplasts of AtCHX23-GFP plants. The green fluorescence of GFP was observed in the envelope membrane vesicles (Fig. 1*D*) but not from the thylakoid vesicles (not shown).

Gene Expression of *AtCHX23*. The expression of *AtCHX23* in different *Arabidopsis* tissues was monitored by the *GUS* reporter gene fused with the *AtCHX23* promoter. The fusion was introduced into *Arabidopsis* by *Agrobacterium*-mediated transformation, and >10 lines were analyzed by histochemical GUS staining. In *AtCHX23* promoter-*GUS* plants, intense GUS staining was observed in the cotyledons, leaves, and sepals (Fig. 2 *A* and *B*). Nongreen tissues (e.g., roots and petals) showed relatively weak expression (Fig. 2 *B* and *D*). RT-PCR analysis using total RNA isolated from different tissues confirmed that *AtCHX23* is expressed in leaves, roots, and stems (Fig. 2*E*).

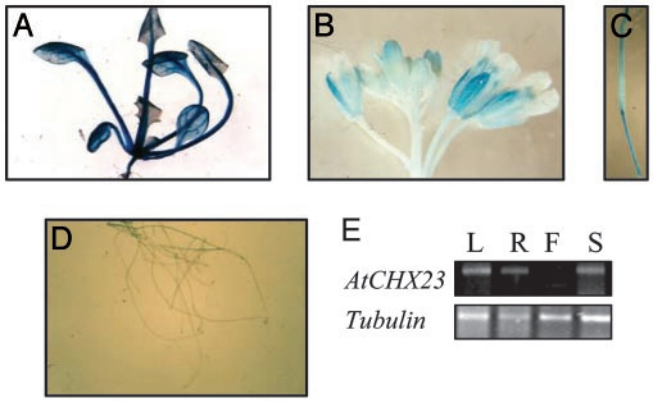

Fig. 2. Histochemical localization of GUS activity directed by *AtCHX23* promoter::GUS fusions in transgenic *Arabidopsis*. (*A*) Transgenic leaves carrying *pAtCHX23-GUS*. (*B*) Transgenic flowers carrying *pAtCHX23-GUS*. (*C*) Silique. (*D*) Transgenic roots carrying *pAtCHX23-GUS*. (*E*) RT-PCR shows the expression of *chx23* in different tissues. L, leaves; R, roots; F, flowers; S, stems.

Loss-of-Function Mutations in *AtCHX23* Impair Chloroplast Development. To determine the function of *AtCHX23*, the gene was silenced by double-stranded RNAi (27) using a cDNA fragment specific to *AtCHX23*. The expression of *AtCHX23* was examined in two independent *chx23* RNAi lines (independent transformants #14 and #20) by using RT-PCR. The results show that *AtCHX23* was silenced in the RNAi lines (Fig. 3*A*). Very interestingly, the RNAi lines showed a strong phenotype in leaf color. Unlike the wild type, which had green cotyledons, the RNAi lines had reddish-purple cotyledons (Fig. 3*B*). Although the leaves of line #14 were all albino (not shown), line #20 could develop yellowish leaves (Fig. 3*B*). The mutant plants have a significantly smaller size compared with wild-type plants and maintain yellowish leaves throughout their life cycle. Smaller

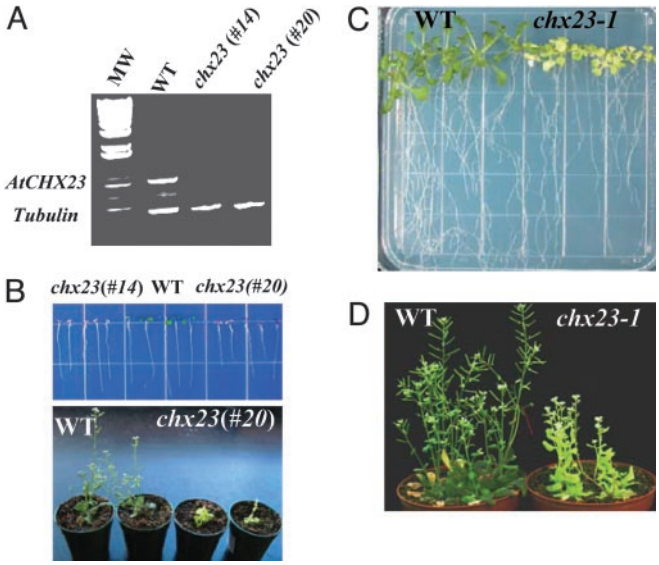

Fig. 3. Phenotype of *chx23* mutants. (*A*) *AtCHX23* gene silencing by double-stranded RNAi. RT-PCR with wild type and two independent lines of *chx23* using *chx23*-specific primers. Tubulin primers were used in PCR as an internal control. (*B*) The seeds of *Arabidopsis* wild type and *chx23* (#14 and #20) were germinated in MS agar medium. The pictures were taken 7 and 20 d after germination and show the phenotype of *chx23* at different developmental stages. (*C*) *chx23-1* mutant from TILLING was germinated in MS for 15 d. (*D*) *chx23-1* grown in soil for 25 d.

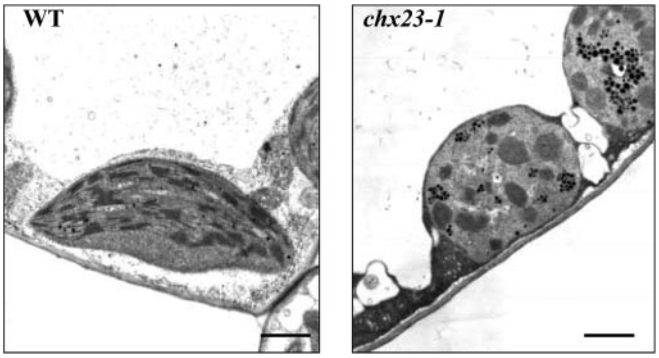

Fig. 4. Ultrastructure of chloroplasts from wild type and the *chx23-1* mutant. All pictures are transmission electron microscope images from ultrathin sections from leaves of 14-d-old seedlings. (Bars = 1 μm.)

siliques and fewer seeds were observed in *chx23* mutant plants, which also require higher humidity to complete their life cycle.

In addition to the RNAi lines, we also identified an ethyl methanesulfonate mutant allele of *AtCHX23*, *chx23–1*, using the targeting induced local lesions in genomes (TILLING) service (http://tilling.fhcrc.org:9366) (28). In the *chx23–1* mutant, a C to T substitution in the fifth exon caused the replacement of Phe-761 by Lys. Like some of the RNAi lines, *chx23–1* mutant plants had yellowish leaves (Fig. 3 *C* and *D*).

Fully grown leaves from wild type and the *chx23–1* mutant were sectioned to examine their chloroplast structure. *chx23–1* mutant leaves have fewer and smaller chloroplasts in the cells (data not shown). Startling morphological changes in plastids in *chx23* mutants were observed by using electron microscopy (Fig. 4). The mutant plastids had straight thylakoids but lacked granal lamellae and contained many densely stained globules, presumably lipid droplets. It is likely that the plastids were thin and twisted, based on the appearance of small, isolated, random thylakoid cross sections within the overall chloroplast structure.

pH-Dependent Chlorophyll Synthesis in *chx23*. We were interested in the potential role of AtCHX23 in modulating the stromal and cytosolic pH in plant cells. As a first attempt, we analyzed the effects of different medium pH values on the amount of chlorophyll in leaves. The seeds of wild type and the *chx23–1* mutant were sown on nutrient media with variation of pH. The *chx23* mutant was very sensitive to high pH (pH 7.0), in which the leaf color became white and the mutant seedlings died after 15 d (Fig. 5*A*). However, at a very low pH (4.0), the growth of *chx23–1* was improved, and the seedlings appeared greener than those in normal pH (5.7). We measured the chlorophyll content at 15 d after germination in the nutrient medium at pH 4.0, 5.7, and 7.0. Chlorophyll of *chx23–1* leaves in plants grown at pH 7.0 was 23% of that at the normal pH of 5.7, whereas chlorophyll in plants grown at pH 4.0 was 139% of that in the controls (Fig. 5*B*). There was little difference in chlorophyll content in wild-type plants grown at the different pH conditions. Thus, the data suggest that AtCHX23 is especially important for coping with high pH, and this is reflected in chloroplast development.

AtCHX23 Is Involved in Regulation of pH Homeostasis. If the *chx23* mutation affects stromal pH, its effect would be reflected in changes in cytosolic pH (pH_{cyt}). Because it was more difficult to measure the stromal pH, we determined the effect of *chx23* mutation on pH_{cyt} as an indication of its effect on stromal pH. When leaves were incubated in the presence of pH probe BCECF-AM and viewed at low magnification (not shown), it was apparent that the vast majority of the BCECF accumulated in

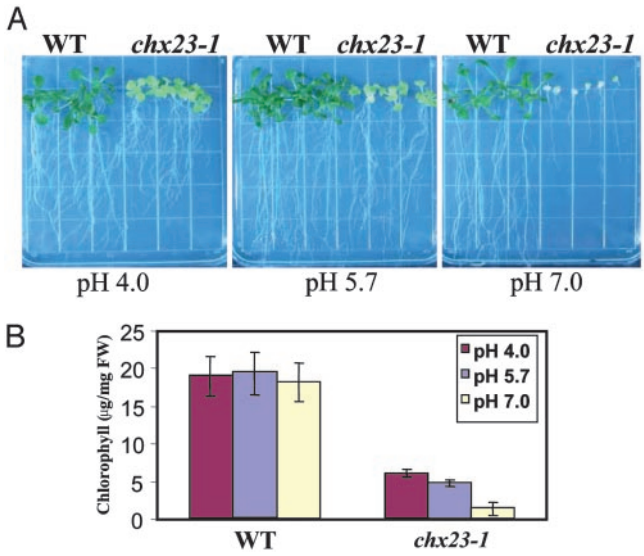

Fig. 5. Effect of pH on *chx23* mutant growth and chlorophyll synthesis. *Arabidopsis* seeds were germinated in MS agar medium at different pH levels (4.0, 5.7, and 7.0). (*A*) Effects of different pH levels on the growth of wild type and *chx23-1*. The pictures were taken 20 d after germination. (*B*) Effects of different pH levels on the chlorophyll content from wild type and *chx23* mutants. Chlorophyll was extracted by using *N*′-dimethylformamide and determined photometrically according to described procedures (29). Presented values are the means from six measurements of six seedlings (15 d) ± SD.

the cytoplasm, which allows the mapping of intracellular pH by confocal fluorescence ratio imaging.

The pH-dependent and -independent fluorescences of BCECF at 535 nm were excited at 488 and 440 nm, respectively. A ratio-vs.-pH curve from *in vivo* calibration was produced in the presence of 100 mM of K^+ and 10 μg/ml nigericin to equilibrate intracellular pH with that of the external solution. It was found that the fluorescence ratio (I_{480}/I_{440}) for BCECF in guard cells varied with changes in pH between 7.0 and 8.0 (Fig. 6*A*).

The average cytoplasmic pH in guard cells of wild-type and *chx23* mutant leaves was estimated by using the above *in vivo* calibration. The results show that the cytoplasmic pH in wild-type guard cells was 7.1, which is a typical pH value for the cytosol. However, the pH value in *chx23–1* guard cells is near 7.4, which is substantially higher than in the wild type (Fig. 6*B*). The ratio images show the pH distribution of guard cells from wild-type and *chx23–1* leaves (Fig. 6*C*). We also determined the cytosolic pH of suspension cells derived from *chx23* mutant and wild-type leaves (data not shown), which produced almost identical results, indicating that cytosolic pH (pH_{cyt}) obtained from guard cells are representative of the normal pH in leaf cells. It is striking that the pH_{cyt} in wild type and *chx23* mutant could differ as much as 0.3 pH units. This means that disruption of AtCHX23 function prevents the acidification or permits a strong alkalization in the cytosol. The results suggest that the stromal pH in *chx23* mutant plants might be lower than normal.

NaCl and KCl Responses in *chx23* Mutants. Because AtCHX23 is a putative Na^+/H^+ or K^+/H^+ antiporter, we tested the effects of Na^+ or K^+ on the growth of the *chx23* mutant. The seeds of wild type and *chx23* were planted in Murashige and Skoog medium (MS medium) containing 75 mM NaCl. *chx23* mutant plants (RNAi line #14) displayed a high sensitivity to NaCl in the medium (Fig. 7*A*). In addition, calli were obtained from wild type and the *chx23* mutant (RNAi line #14) by culture of leaves in MS medium containing 2,4-D and kinetin. No significant difference in growth was observed between wild-type and *chx23*

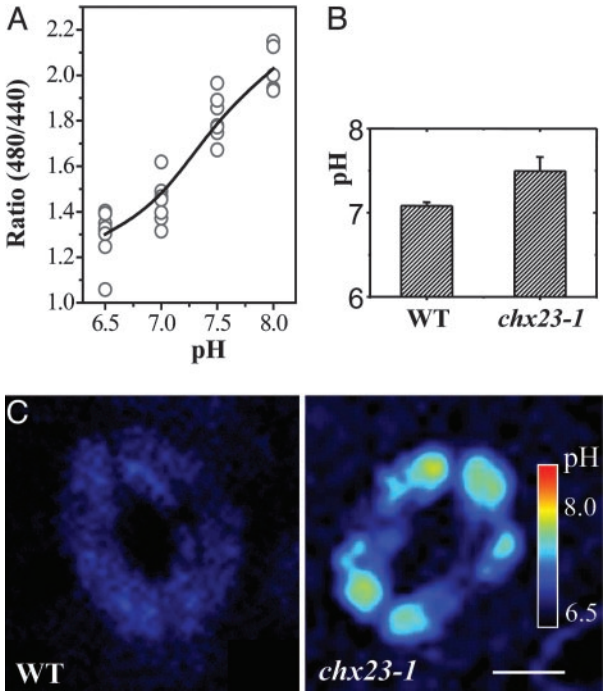

Fig. 6. Cytoplasmic pH in wild-type and *chx23* plants. (*A*) *In situ* calibration was performed by using 10 μg/ml nigericin and 100 mM KCl in buffers of different pH. Pixel values were averaged over recticular regions (15–30 μm^2) manually located on each wavelength image. A single ratio value was calculated from the average 488 intensity divided by the average 442 intensity for this region, after subtraction of the corresponding image backgrounds. Values >200 were masked in both images to exclude pixels approaching saturation. (*B*) The pH changes in guard cells of wild type and *chx23-1*. The conversion from ratio values to pH derived from the *in vivo* calibration is indicated as the average cytosolic pH (mean ± SD, n = 8 cells). (*C*) pH distribution of guard cells was monitored by pseudoratiometric confocal imaging of the fluorescence from the pH-sensitive dye BCECF-AM through dual-excitation confocal ratio measurement. The pseudocolor bar in *C* represents a pH range from ≈8.0 to 6.5. (Bar = 10 μm.)

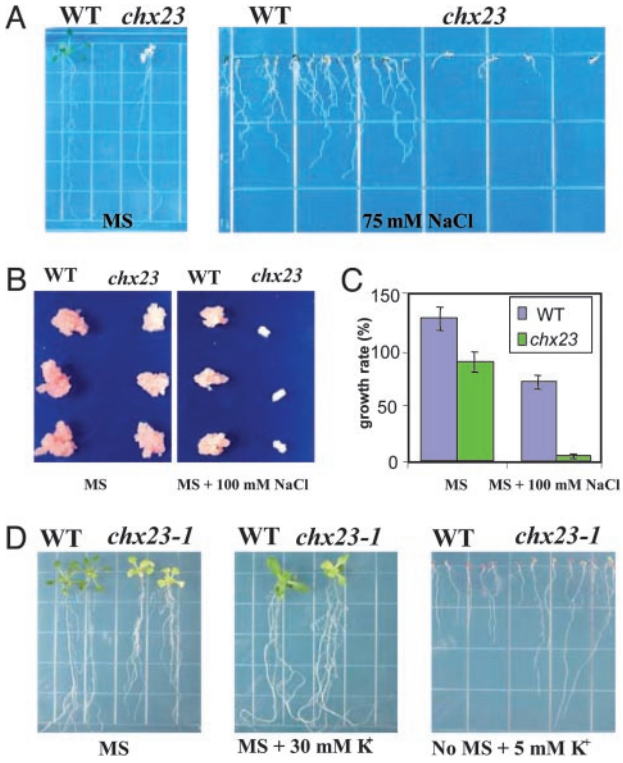

Fig. 7. The effects of NaCl and KCl on the phenotype of *chx23* mutants. (*A*) The germination of seeds from wild type and *chx23* mutants. The pictures were taken 12 d after germination in MS agar plates without or with 75 mM NaCl. (*B*) Effects of NaCl on relative growth rate of wild type and *chx23* mutant calli. Callus was generated from seedlings of the wild type and mutants, by incubation on callus-initiating medium containing MS salts, 2% sucrose, 3 mg/liter 2,4-D, 50 μg/liter and 0.8% agar for 2 weeks. (*C*) Effects of NaCl on relative growth rate of *Arabidopsis* calli. Calli were incubated in the corresponding medium for 24 d. Data are the means ± SD of three independent experiments with three replicates per experiment. (*D*) Wild-type and *chx23* plants grown in MS medium or MS supplemented with 30 mM KCl or no MS salts supplemented with 5 mM KCl.

mutant calli (Fig. 7*B*). However, *chx23* calli showed slower growth than wild type in the same medium supplemented with 100 mM NaCl (Fig. 7 *B* and *C*).

We also planted wild type and *chx23-1* in MS media with or without KCl supplementation. In the MS medium supplemented with 30 mM KCl, *chx23–1* grew nearly as well as the wild-type plants (Fig. 7*D*). Interestingly, with only 5 mM KCl in the medium, the roots of *chx23–1* grow faster than wild-type plants. Consistent with a role of AtCHX23 in ion transport, guard cells of *chx23–1* mutant leaves show a larger response to added KCl than wild type. In stomatal opening buffer containing 100 mM KCl, *chx23–1* mutant epidermal peels showed wider stomatal aperture than that of the wild type (data not shown). The average stomatal aperture of wild-type plants in the light was increased by KCl to 123% of that without potassium; in the *chx23* mutant, it increased to 194%.

Discussion

Earlier biochemical and physiological data suggested that an unknown $Na^+(K^+)/H^+$ antiporter is localized in the chloroplast envelope, partially regulating stromal acidification and alkalization (7, 8, 30). The stroma pH level is an important factor for high photosynthetic activity. Our results presented here suggest that AtCHX23, probably the hypothetical $Na^+(K^+)/H^+$ antiporter of the chloroplast envelope, plays an important role in cytoplasmic and possibly stromal pH regulation and in chloroplast development. The chloroplast localization of AtCHX23 is supported by the observed site of the AtCHX23-GFP fusion protein green fluorescence signal (Fig. 1). Purification of intact chloroplasts on a Percoll gradient, followed by isolation of the envelopes, provided further evidence for localization of the gene product. It is not surprising that AtCHX23 appears to be most similar to NhaS3, a Na^+/H^+ antiporter in *Synechocystis*. This phylogenetic relationship is consistent with the generally accepted endosymbiotic hypothesis, which states that chloroplasts arose from an internalized cyanobacterial ancestor (31).

Because the AtCHX23 protein is likely a neutral Na^+ (or K^+)/H^+ antiporter, its effects will vary with the relative cation and proton concentrations on either side of the chloroplast envelope. In the dark, with cytoplasmic and stromal pH values close to equal, relatively little flux through this antiporter would be expected. In the light, as the stroma pH becomes more alkaline than that of the cytosol, a flux of monovalent cations (Na^+ or K^+) from the cytosol into the stroma through AtCHX23 would permit proton loss, thereby maintaining a high stroma pH. Consistent with such a role of AtCHX23, we found that the cytoplasmic pH in *chx23* mutant is higher than from wild type (Fig. 6).

The abnormal leaf color and chloroplast internal structure produced in *chx23–1* mutant leaves show that the mutant is impaired in chloroplast development. The pleiotropic effects of the *AtCHX23* mutation could start by interfering with the ion

homeostasis and therefore the function of the plastids. This could include leucoplasts in the root and proplastids in germinating seedlings. Plastids, of course, do much more for the plant than photosynthesize. The metabolism located in plastids includes synthesis of about half of the cell's amino acids, as well as of many of the specific lipids, carotenoids, purines, and pyrimidines. Conditions that impair an unknown number of these functions will inevitably lead to wide disturbances in the biochemistry and physiology of the plant.

The loss of the envelope antiporter makes the *chx23* mutant highly sensitive to NaCl. A partial explanation might be that in the wild type, a considerable part of entering Na^+ ions are sequestered in chloroplasts, due to the activity of the normal AtCHX23 Na^+/H^+ antiporter. Without the antiporter, the cytosol might suffer more from Na^+ ion toxicity. Compartmentalization of Na^+ into the chloroplasts might be effective, because there are so many chloroplasts in plant cells. This mechanism could be especially important in sugar beet, where chloroplasts often contain a high concentration of Na^+, and Na^+ and K^+ are incorporated in the chloroplasts to a similar extent (32); also, Na^+ was able to replace K^+ for chloroplast multiplication (33). This might also be true for *Limonium vulgare*, in which the chloroplast Na^+ content was reported to be even higher than K^+ (32). Although most plants have been reported to have a low Na^+ content in chloroplast stroma, it is possible that sequestration of this ion into chloroplasts occurs as a partial detoxification mechanism in *Arabidopsis* or most other plants.

Our observation that *chx23* has faster growth (Fig. 7*D*) and more chlorophyll content (Fig. 5) in MS medium supplemented with 30 mM KCl than that in MS without extra KCl indicates that AtCHX23 might also function in K^+ transport. The process that is generally regarded as being the most sensitive to K^+ is the maintenance of turgor pressure and, as a consequence, cell expansion. Therefore, accumulated cytosolic potassium resulting from the defective *chx23* might permit faster growth of the mutant (34). The stomatal opening in *chx23–1* leaves was also more stimulated by external K^+ than in wild type (data not shown). K^+ is the dominant cation responsible for turgor change in guard cells during ion-induced stomatal movement. The stronger effect of K^+ on the mutant suggests there may be more K^+ available in the *chx23–1* cytoplasm for stomatal opening, possibly due to defective K^+ loading into the chloroplasts as a consequence of the *chx23–1* mutation.

We thank Mr. P. Wang (Henan University, Kaifeng, China) and D. Bentley (University of Arizona, Tucson) for help in the analysis of pH images. This work was supported by National Institutes of Health Grant R01GM59138 and by U.S.–Israel Binational Agricultural Research and Development Fund Grant IS-2971-98 (to J.-K.Z.).

1. Mitchell, P. (1961) *Nature* **191,** 144–148.
2. Jagendorf, A. T. & Uribe, A. T. (1966) *Proc. Natl. Acad. Sci. USA* **55,** 170–177.
3. Werdan, K., Heldt, H. W. & Milovancev, M. (1975) *Biochim. Biophys. Acta* **396,** 276–292.
4. Heldt, H. W., Wedan, K. W., Milovancev, M. & Geller, G. (1973) *Biochim. Biophys. Acta* **314,** 224–241.
5. Felle, H. H. (2001) *Plant Biol.* **3,** 577–591.
6. Demming, B. & Gimmler, H. (1983) *Plant Physiol.* **73,** 169–174.
7. Huber, S. C. & Maury, W. (1980) *Plant Physiol.* **65,** 350–354.
8. Peters, J. S. & Berkowitz, G. A. (1991) *Plant Physiol.* **95,** 1229–1236.
9. Wu, W. & Berkowitz, G. A. (1992) *Plant Physiol.* **98,** 666–672.
10. Padan, E., Venturi, M., Gerchman, Y. & Dover, N. (2001) *Biochim. Biophys. Acta* **1505,** 144–157.
11. Apse, M. P., Aboron, G. S., Snedden, W. A. & Blumwald, E. (1999) *Science* **285,** 1256–1258.
12. Fukada-Tanaka, S., Inagaki, Y., Yamaguchi, T., Saito, N. & Iida, S. (2000) *Nature* **407,** 581.
13. Numata, M., Petrecca, K., Lake, N. & Orlowski, J. (1998) *J. Biol. Chem.* **273,** 6951–6959.
14. Shi, H., Ishitani, M., Kim, C. & Zhu, J.-K. (2000) *Proc. Natl. Acad. Sci. USA* **97,** 6896–6901.
15. Gaxiola, R. A., Li, J., Undurraga, S., Dang, L. M., Allen, G. J., Alper, S. L. & Fink, G. R. (2001) *Proc. Natl. Acad. Sci. USA* **98,** 11444-11449.
16. Apse, M. P., Sottosanto, J. B. & Blumwald, E. (2003) *Plant J.* **36,** 229–239.
17. Yamaguchi, T., Fukada-Tanaka, S., Inagaki, Y., Saito, N., Yonekura-Sakakibara, K., Tanaka, Y., Kusumi, T. & Iida, S. (2001) *Plant Cell Physiol.* **42,** 451–461.
18. Qiu, Q. S., Guo, Y., Dietrich, M. A., Schumaker, K. S. & Zhu, J.-K. (2002) *Proc. Natl. Acad. Sci. USA* **99,** 8436–8441.
19. Shi, H., Quintero, F. J., Pardo, J. M. & Zhu, J.-K. (2002) *Plant Cell* **14,** 465–477.
20. Mäser, P., Thomine, S., Schroeder, J. I., Ward, J. M., Hirschi, K., Sze, H., Talke, I. N., Amtmann, A., Maathuis, F. J. M., Sanders, D., *et al.* (2001) *Plant Physiol.* **126,** 1646–1667.
21. Murashige, T. & Skoog, F. (1962) *Physiol. Plant.* **15,** 473–497.
22. Kunst, L. (1988) *Methods Mol. Biol.* **82,** 43–48.
23. Froehlich, J. E., Itoh, A. & Howe, G. A. (2001) *Plant Physiol.* **125,** 306–317.
24. Fricker, M. D., White, N. S. & Obermeyer, G. (1997) *J. Cell Sci.* **110,** 1729–1740.
25. Swanson, S. J. & Jones, R. L. (1996) *Plant Cell* **8,** 2211–2221.
26. Elanskaya, I. V., Karandashova, I. V., Bogachev, A. V. & Hagemann, M. (2002) *Biochemistry* **67,** 432–440.
27. Chuang, C. F. & Meyerowitz, E. M. (2000) *Proc. Natl. Acad. Sci. USA* **97,** 4985–4990.
28. McCallum, C. M., Comai, L., Greene, E. A. & Henikoff, S. (2000) *Nat. Biotechnol.* **18,** 455–457.
29. Porra, R. J., Thompsin, W. A. & Kriedman, P. E. (1989) *Biochim. Biophys. Acta* **975,** 384–394.
30. Maury, W. J., Huber, S. C. & Moreland, D. E. (1981) *Plant Physiol.* **68,** 1257–1263.
31. Cavalier-Smith, T. (2000) *Trends Plant Sci.* **5,** 174–182.
32. Subbarao, G. V., Wheeler, R. M., Berry, W. L. & Stutte, G. W. (2002) *Handbook of Plant and Crop Physiology*, ed. Pessarakli, M. (Dekker, New York), 2nd Ed., pp. 363–384.
33. Marschner, H. (1971) in *Proceedings of 8th Colloquium of International Potash Institute (Berlin)*, pp. 50–63.
34. Hsiao, T. C. & Lauchli, A. (1986) *Adv. Plant Nutr.* **2,** 281–312.